Int. J. Electrochem. Sci., 14 **(2019)** 6555 – 6570, doi; 10.20964/2019.07.36

International Journal of ELECTROCHEMICAL SCIENCE
www.electrochemsci.org

Corrosion Inhibition Effect of N-benzyl-N-(2,4-diamino) butyl imidazoline ammonium chloride on mild steel in 1.0 M HCl solution

Honghong Zhang[1,2,*], *Yu Chen*[2,*], *Zhongnian Yang*[2]

[1] Department of Chemistry, Zhejiang University, Hangzhou, Zhejiang 310027, China
[2] Department of Chemical Engineering and Safety, Binzhou University, Binzhou, Shandong 256600, China
[*]E-mail: bzuzhanghong@163.com (Honghong Zhang); chen123yu123@163.com (Yu Chen)

Received: 17 March 2019/ *Accepted:* 30 April 2019 / *Published:* 10 June 2019

Novel imidazoline derivative, named N-benzyl-N-(2,4-diamino) butyl imidazoline ammonium chloride (BIA) based on soybean oil was synthesized and its structure was characterized by FTIR. The inhibition behavior of BIA inhibitor for mild steel in 1.0 M HCl was investigated using gravimetric measurements, potentiodynamic polarization, electrochemical impedance spectroscopy (EIS), scanning electron microscopy (SEM) and energy dispersive spectrum. Both the gravimetric results and SEM studies revealed that BIA acted as an efficient inhibitor for mild steel in 1.0 M HCl solution. Gravimetric measurements suggested that the corrosion rate decreased with the increase of inhibitor concentration and the inhibition efficiency reached the maximum value of 96.4% at 200 mg/L. Potentiodynamic polarization results demonstrated that the synthesized imidazoline derivative performed as mixed-type inhibitor, predominantly cathodic.Adsorption of BIA inhibitor on mild steel surface in 1.0 M HCl solution was spontaneous and conformed to Langmuir adsorption isotherm and the adsorption free energy was found to be -22 kJ/mol. Meanwhile, some thermodynamic parameters (E_a, ΔH^*, ΔS^*) were calculated and discussed.

Keywords:mild steel; inhibition; polarization; EIS

1. INTRODUCTION

Mild steel has been widely used as structural material in industry [1-3]. However, they will be easily corroded when exposed to HCl solution, which is commonly applied in industrial cleaning to remove undesirable scale and rust. The utilization of organic compounds has been found to be an efficient and practical method to protect mild steel from corrosion in acidic media [4-7]. The inhibition performance does not only relate to the corrosive media, but also the structure of organic compounds.

It is well known that the most popular inhibitors often contain nitrogen, sulfur, oxygen, heterocyclic/aromatic rings or polar functional groups [8-10], which acts as adsorption centers to form a protective film on the mild steel surface.

However, the addition of large quantities of these organic compounds may bring undesirable toxicity to the environment and human, which undoubtedly limited their wide application. Thus, looking for "green" and "non-toxic" organic inhibitors becomes urgent and significant. Great efforts have been made for researchers and some natural products, such as plant extracts [11-16], vegetable oils and its derivatives [17-19] have attracted much more interest for their low cost and environmental friendless. Thymus vulgaris plant extract has been used as an eco-friendly corrosion inhibitor for stainless steel 304 in 1.0 M HCl solution [14]. The Tiliacordata extract presented a high inhibition efficiency of 96% at 300 mg/L for carbon steel in acidic solutions [16]. Soybean oil is a normal vegetable oil and rich in Heilongjiang province of China which can be used as a green chemical source for preparation of organic inhibitor.

Based on the consideration that organic compounds with N, O, P and heterocyclic rings can be used as excellent inhibitors for mild steel in acidic solution, a novel imidazoline derivative based on soybean oil was synthesized in this work and the inhibition effect on mild steel in 1.0 M HCl solution was systematically studied by gravimetric measurements, potentiodynamic polarization, electrochemical impedance spectroscopy (EIS), scanning electron microscopy (SEM) and energy dispersive spectrum (EDS). The effects of inhibitor concentration, testing temperature and immersion time on the inhibition efficiency were also evaluated.

2. EXPERIMENTAL

2.1 Materials

The corrosive media of 1.0 M HCl solution was prepared from diluting the analytical grade 37 wt.% HCl with double distilled water. The imidazoline derivative based on soybean oil was synthesized according to the scheme presented in Fig.1. Firstly, soybean oil (3B Pharmachem International Co., Ltd.) was reacted with triethylenetetramine (Sinopharm Chemical Reagent Co., Ltd.) at 140-160 °C under magnetic stirring for 4.5 h. Secondly, the obtained product was heated up to 200-210 °C and refluxed until the theoretical amount of water was collected in a Dean-Stark trap. The dehydration process was detected by thin layer chromatography (TLC). Thirdly, the dehydrated mixture was reacted with benzyl chloride (Sinopharm Chemical Reagent Co., Ltd.) at about 110 °C for about 3 h to complete the quaterisation. Finally, the raw product was purified by column chromatography with the mixture of trichloromethane and ethyl acetate.

The structure of the purified product N-benzyl-N-(2,4-diamino) butyl imidazoline ammonium chloride (designated as BIA) was characterized by FTIR (Nexus670, NICOLET) in the wave-number range from 400 to 4000 cm^{-1}, and the result was shown in Fig.2. Two peaks located at 2924 cm^{-1} and 2853 cm^{-1} are observed for both soybean oil and the obtained BIA, which correspond to the asymmetric stretching and symmetric stretching vibration of C-H. It is noticeable that a strong

absorption peak at 1600 cm^{-1} appeared for obtained BIA, which was correlated to the C=N bond in the imidazole ring. Meanwhile, the peak at 3298 cm^{-1} may be due to N-H. Another peak located at 703 cm^{-1} corresponds to single substitution in benzene ring. From the above analysis, it is rational to deduce that the target compound had been synthesized.

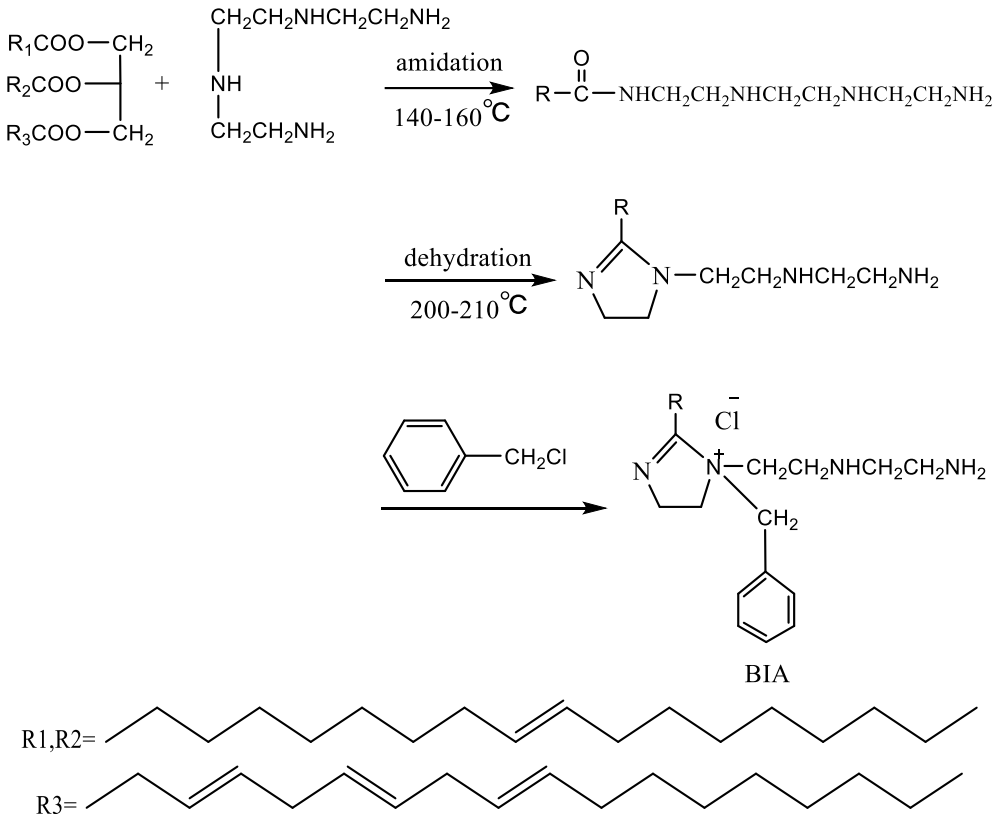

Figure 1. Preparation scheme of N-benzyl-N-(2,4-diamino) butyl imidazoline ammonium chloride (BIA).

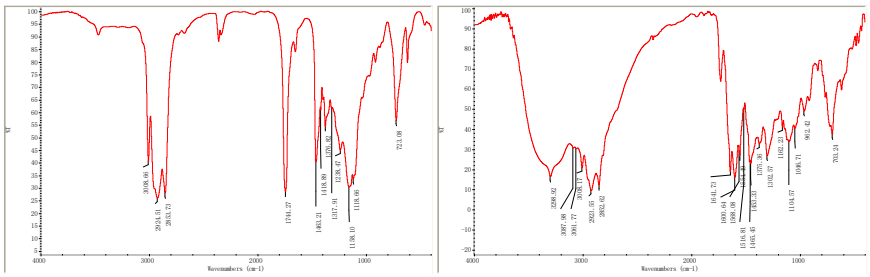

Figure 2. FTIR of the (a) soybean oil; (b) obtained BIA.

2.2 Weight loss experiments

The weight loss experiments were conducted using mild steel samples of dimension 50 mm × 25 mm × 5 mm and the chemical composition was shown in Table 1. Before experiments, the mild steel samples were successively abraded with different grit emery papers, washed in acetone, rinsed

with double distilled water and then immersed into 1.0 M HCl solution without and with different concentration of BIA inhibitor. After 8 h immersion time, the mild steel samples were moved out, carefully cleaned and accurately weighted. The corrosion rate (mg cm^{-2} h^{-1}), inhibition efficiency (*IE%*) and surface coverage (θ) were calculated using the following equations [20]:

$$C_R = \frac{87.6 \times W}{A \times t \times \rho} \quad (1)$$

$$IE(\%) = (1 - C_{Rinhi}/C_{R\,free}) \times 100 \quad (2)$$

$$\theta = 1 - C_{Rinhi}/C_{R\,free} \quad (3)$$

where W is the mass loss (mg), A is the working area in cm^2, t is 8 h and ρ is the density (7.86×10^3 g cm^{-3}).$C_{R\,inhi}$ and $C_{R\,free}$ correspond to the calculated corrosion rate for mild steel with and without inhibitors, respectively.

Table 1. Chemical composition (mass fraction, wt. %) of Q235 mild steel samples.

C	Mn	Si	S	P	Fe
0.16	0.53	0.30	<0.055	<0.045	Bal.

2.3 Electrochemical measurements

A conventional three electrode electrolytic cell was used to take out the electrochemical tests. The cylindrical mild steel with an exposed area of 0.50 cm^2, a large platinum sheet, and a saturated calomel electrode (SCE) served as the working, auxiliary and reference electrode, respectively. Prior to electrochemical measurements, the working electrode was polished to mirror using 2.5 μm diamond paste, and then degreased in acetone. The working electrode was immersed into the testing solution without and with different concentration of BIA inhibitor for 1 h to reach a steady state of the open circuit potential (OCP). Potentiodynamic polarization curves were performed in the potential range from E_{ocp}-250 mV to E_{ocp}+250 mV at a scanning rate of 1 mV/s. EIS spectra were recorded over the frequency range from 100 KHz to 10 mHz at E_{ocp} with AC amplitude of 5 mV using an impedance measurement unit (PARSTAT 2273).

2.4 Surface investigation

The surface morphologies of mild steel samples in 1.0 M HCl solution in the absence and presence of BIA inhibitor were observed using SEM model Hitachi SU80 at an accelerating voltage of 30 kV. The surface composition was further investigated using EDX detector model coupled with SEM.

3. RESULTS AND DISCUSSION

3.1 Weight loss measurements

Table 2. The weight loss parameters for mild steel in 1.0 M HCl solution at 30 °C in the absence and presence of different concentrations of BIA inhibitor.

c(mg/L)	C_R(mg cm^{-2} h^{-1})	η(%)	Θ
0	4.78	-	-
50	0.564	88.2	0.882
100	0.354	92.6	0.926
150	0.258	94.6	0.946
200	0.172	96.4	0.964
250	0.177	96.3	0.963

The inhibition effect of BIA inhibitor on mild steel in 1.0 M HCl solution at 30 °C was studied using gravimetric measurements and the results are given in Table 2. Obviously, the corrosion rate decreases with addition of BIA inhibitor compared to the blank, which value decreases with increasing BIA inhibitor concentration. Accordingly, the inhibition efficiency increases with the increase of BIA inhibitor concentrations from 50 mg/L to 200 mg/L, which may be related to the adsorption of BIA inhibitor molecules at the mild steel surface. The value of inhibition efficiency reaches up to a maximum value of 96.4% at the concentration of 200 mg/L, suggesting that the synthesized BIA acts as an excellent corrosion inhibitor for mild steel in 1.0 M HCl solution. Noticeably, the inhibition efficiency changes little when the BIA inhibitor concentration increases from 200 mg/L to 250 mg/L.

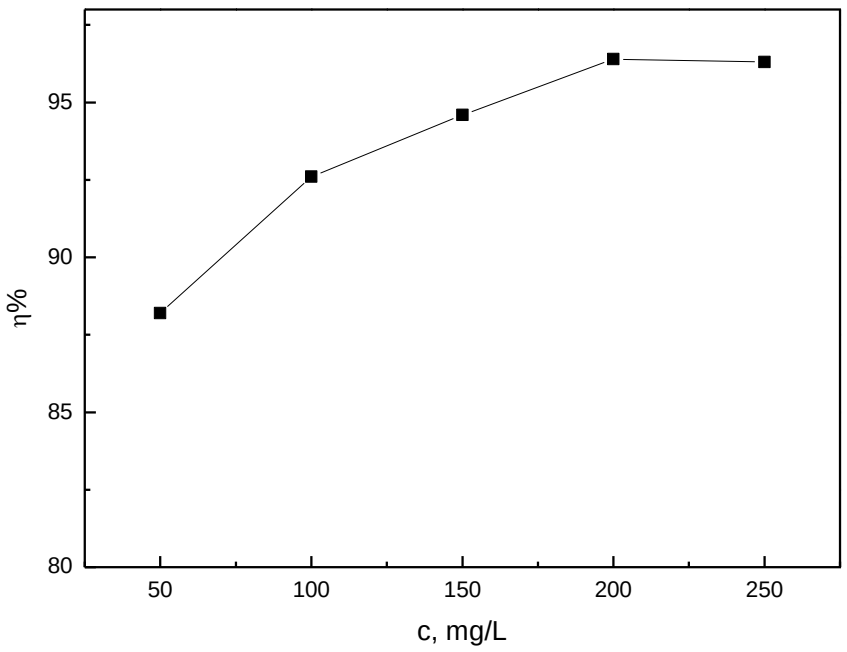

Figure 3. Dependence of inhibition efficiency on BIA inhibitor concentration.

3.2 Potentiodynamic polarization curves

The typical potentiodynamic polarization curves for mild steel corrosion in 1.0 M HCl solution without and with different concentrations of BIA inhibitor are presented in Fig.4. It is clear that the current densities of both the anodic and cathodic branches decrease in the presence of BIA inhibitor compared to the uninhibited sample, which may be ascribed to the coverage of inhibitor molecules on mild steel surface. In addition, the shape of potentiodynamic polarization curves changes little with addition of BIA inhibitor, suggesting that BIA inhibitor suppressed the mild steel dissolution by adsorption at the active sites on its surface and did not change the dissolution mechanism [21]. It also can be seen that the E_{corr} moves to the negative direction with addition of BIA inhibitor. Some electrochemical parameters, including corrosion current density (j_{corr}), corrosion potential (E_{corr}), cathodic and anodic Tafel slopes were obtained by Tafel extrapolation method and summarized in Table 3.

The inhibition efficiency η_P(%) can be calculated using the following equation [22,23], which values were also listed in Table 3.

$$\eta_P\% = (1 - j_{inhi} / j_{free}) \times 100\% \qquad (4)$$

Where j_{inhi}andj_{free} are the corrosion current densities for the inhibited and uninhibited samples, respectively.

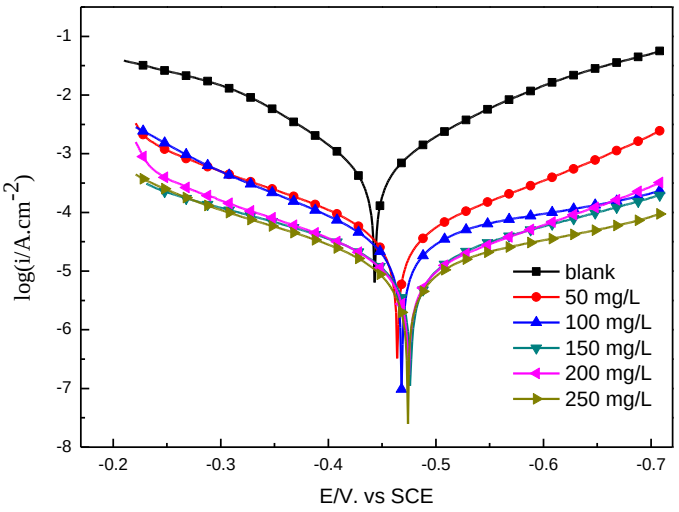

Figure 4. Polarization plots for mild steel in 1.0 M HCl solution without and with different concentrations of BIA inhibitor.

The inspection of Table 4 suggests that the maximum shift in E_{corr} is 25 mV, which value is less than 85 mV, indicating that the synthesized BIA is a mixed-type inhibitor [24]. Additionally, a more pronounced change can be observed in the value of β_c, revealing that BIA inhibitor is predominantly cathodic. The value of I_{corr} decreases from 496 μA cm^{-2} to 40.7 μA cm^{-2} when the BIA inhibitor concentration increases from 0 to 200 mg/L, suggesting that BIA compound is an efficient inhibitor for mild steel in 1.0 M HCl solution.

Table 3. Polarization parameters for mild steel in 1.0 M HCl solution without and with different concentrations of BIA inhibitor.

c(mg/L)	E_{corr} (mV)	β_a (mV dec^{-1})	$-\beta_c$ (mV dec^{-1})	i_{corr} (μA cm^{-2})	η_P(%)
0	-443	95	108	496	-
50	-459	137	147	78.9	84
100	-468	131	151	67.5	86
150	-475	165	178	52.1	90
200	-474	146	260	40.7	92
250	-478	156	234	41.7	92

3.3 EIS measurements

Fig.5 shows the typical Nyquist diagrams for mild steel corrosion in 1.0 M HCl solution without and with different concentrations of BIA inhibitor. It is clear that the addition of BIA inhibitor has a great influence on the Nyquist plots and the diameter increases significantly compared to the blank. This phenomenon suggests that the dissolution rate of mild steel in 1.0 M HCl solution was remarkably restrained by BIA inhibitor. With increasing BIA inhibitor concentration, the diameter of the capacitive circle increases, indicating the formation of a more compact protective film on mild steel surface. As deduced through both the EIS diagram features and the method proposed by Wit [25,26], the impedance spectra consists of only one depressed capacitive loop in the blank solution while two in the presence of BIA inhibitor. These two capacitive loops located at high frequency and middle frequency are ascribed to the double layer capacitance and film capacitance, respectively. In addition, the Nyquist plots are not ideal semicircles and this may be due to the dispersion effect at the solid/ liquid interface, which is originated from the surface roughness and chemical inhomogeneity [27]. Thus, the electrochemical equivalent circuit as shown in Fig.6 was used to simulate the EIS data. In this equivalent circuit, the impedance of CPE can be represented as follows [28-30]:

$$Z_{CPE} = \frac{1}{Y_0 (j\omega)^n} \qquad (5)$$

where ω is the angular frequency, and n is a CPE exponent which represents the surface roughness [31].

The fitted results are listed in Table 4. The inhibition efficiency derived from EIS measurements can be calculated with the following equation [32], whose results are also listed in Table 4.

$$IE(\%) = (1 - R_p^{free} / R_p^{inhi}) \times 100 \qquad (6)$$

Where R_p^{free} and R_p^{inhi} are the total resistance without and with different concentration of BIA inhibitor, respectively.

From Table 4, it can be seen that both R_f and R_{ct} increases with increasing BIA inhibitor concentration, suggesting the adsorption of BIA molecules on mild steel surface. The highest value of R_{ct} has been found to be 593 Ω cm^2 at the concentration of 200 mg/L. Meanwhile, the value of Q_{dl}

decreases with the increase of inhibitor concentrations, which may be due to the replacement of pre-adsorbed water molecules by BIA compound [33]. This finding further proved the adsorption of BIA inhibitor on mild steel surface. Moreover, the values of *n* are a little larger with addition of BIA inhibitor than that of blank, indicating that the mild steel surface becomes smooth in the presence of BIA due to the formation of protective film.

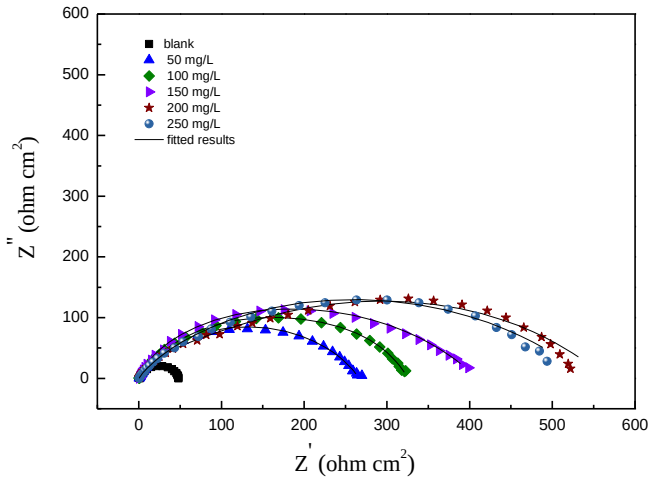

Figure 5. Nyquist impedance diagrams of mild steel in 1.0 M HCl solution containing different concentrations of BIA inhibitor.

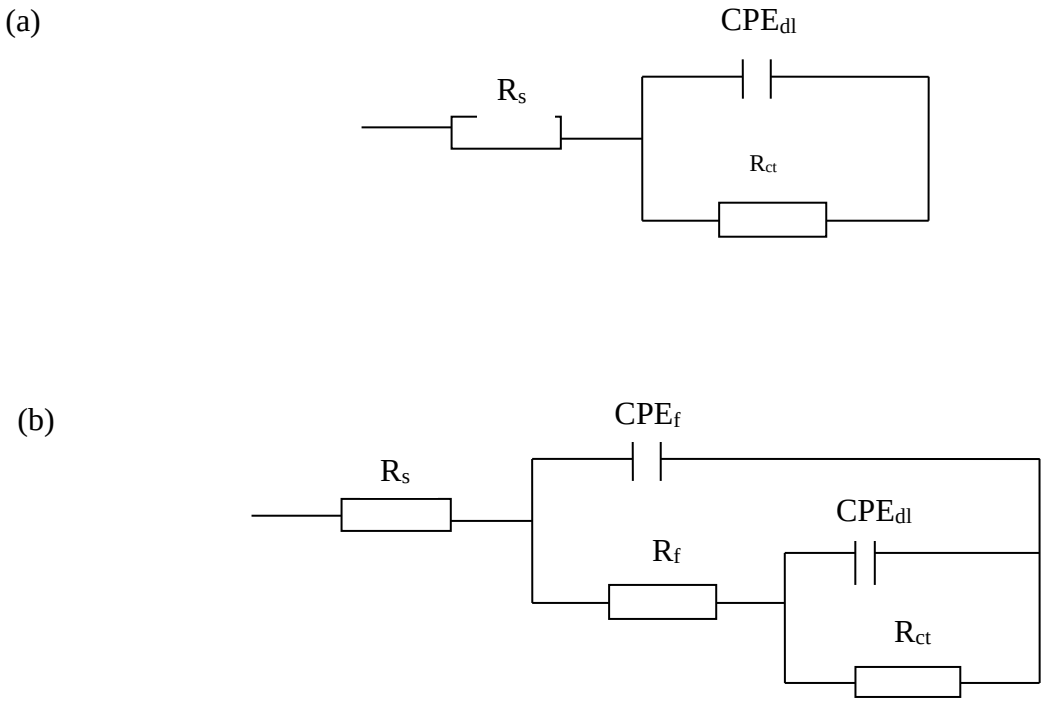

Figure 6. Equivalent electrochemical circuit model used to simulate the EIS data. (a) R_s is solution resistance, $CPE_{dl}$and R_{ct} correspond to double layer capacitance and charge transfer resistance, respectively. (b) $CPE_f$and R_f represents the film capacitance and film resistance, respectively.

Table 4. EIS parameters for Q235 mild steel in 1.0 M HCl solution without and with different concentrations of BIA inhibitor.

c(mg/L)	R_s (Ω cm^2)	R_f (Ω cm^2)	R_{ct} (Ω cm^2)	Q_{dl} ($\Omega^{-1}s^n$ cm^{-2})	$R_p=R_f+R_{ct}$ (Ω cm^2)	n_{dl}	η_{EIS} (%)
0	1.32	-	33.8	204	33.8	0.91	-
50	1.76	21.0	243	128	264	0.95	87.2
100	1.46	28.3	297	117	325	0.94	89.6
150	1.48	34.4	405	105	439	0.96	92.3
200	1.17	48.5	544	94	593	0.97	94.3
250	1.74	45.9	490	98	536	0.95	93.7

3.4 Surface investigation

The surface morphologies of mild steel after immersion in 1.0 M HCl solution in the absence and presence of 200 mg/L BIA inhibitor are shown in Fig.7.

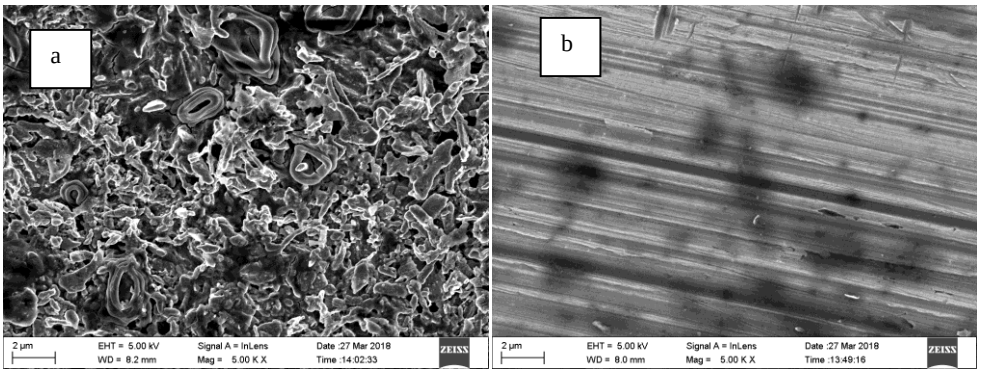

Figure 7. SEM images of mild steel surface without out (a) and with 200 mg/L BIA inhibitor (b) in 1.0 M HCl solution.

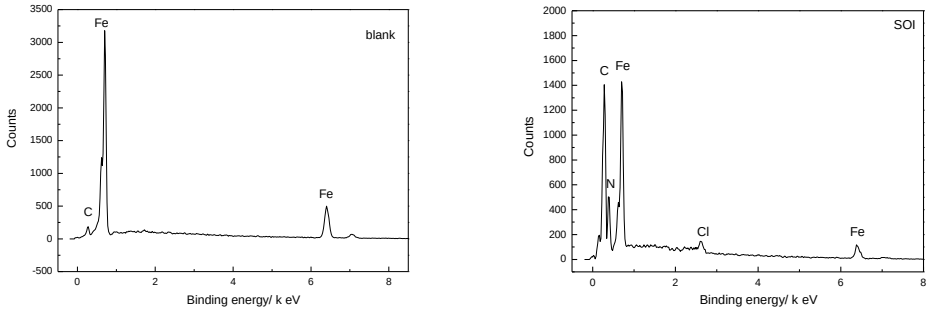

Figure 8. EDX spectra of mild steel samples in1.0 M HCl solution without and with 200 mg/L BIA inhibitor.

It is apparent that the mild steel surface was remarkably destroyed without BIA inhibitor (Fig.7a), while the mild steel surface with addition of 200 mg/L BIA inhibitors was much more uniform (Fig.7b), suggesting that the adsorption of BIA inhibitor on mild steel surface supplied an

protective barrier to restrain the aggressive attack of acidic media. EDX spectra were conducted to study the change of chemical composition (Fig.8). No characteristic peaks for nitrogen (N) and chlorine (Cl) were observed in the uninhibited 1.0 M HCl solution, while these two peaks appeared with addition of 200 mg/L BIA inhibitor. This phenomenon indicated the presence of BIA molecules on mild steel surface.

3.5 Adsorption isotherm

It is well known that the organic reduces steel dissolution through adsorption at the steel/solution interface and the adsorption isotherm can give deep insights into the correlation between organic molecules and steel surface. Therefore, some adsorption isotherms, such as Langmuir, Frumkin and Temkin isotherms, were employed to simulate the relationship between BIA inhibitor concentration (c) and surface coverage (θ) obtained from weight loss measurements. As plotted in Fig.9, the dependence of c/θ on c yielded a straight line, indicating that the adsorption of BIA inhibitor on mild steel surface was best fitted to the Langmuir adsorption isotherm [34-36]:

$$\frac{c}{\theta} = \frac{1}{K_{ads}} + c \qquad (7)$$

Where c is inhibitor concentration, θ is surface coverage and K_{ads} is the equilibrium constant for the adsorption/desorption process of BIA inhibitor on mild steel surface.

Moreover, the standard free energy of adsorption ΔG_{ads}^0 can be calculated according to the following relation [37]:

$$-\Delta G_{ads}^0 = -RTln(55.5K_{ads}) \qquad (8)$$

Where R is the universal gas constant and T is the absolute temperature.

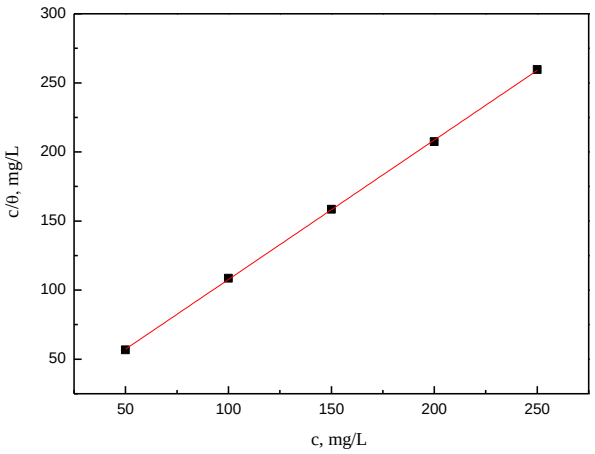

Figure 9. Langmuir adsorption isotherm for BIA inhibitor adsorption on to mild steel surface.

The value of ΔG_{ads}^0 was calculated to be -22 kJ/mol. The negative value suggests the spontaneous adsorption of BIA inhibitor on mild steel surface [38]. According to the previous study, the value of ΔG_{ads}^0 around -20 kJ/mol or lower demonstrates the physical adsorption mechanism through electrostatic interaction, whereas around -40 kJ/mol or higher suggests the chemical

adsorption mechanism involving charge transfer or sharing to form a coordinate type of bond [39]. Thus, it is rational to conclude that the adsorption of BIA inhibitor on mild steel surface involves both physisorption and chemisorption and physical adsorption is the predominant mode.

3.6 Effect of temperature

The effect of temperature ranging from 30 °C to 60 °C on the corrosion behavior of mild steel in 1.0 M HCl solution in the absence and presence of 200 mg/L BIA inhibitor was studied with gravimetric measurements and the results are summarized in Table 5. It can be seen that the value of C_R increases from 4.78 to 28.5 mg cm^{-2} h^{-1} with rising temperature from 30 °C to 60 °C in the absence of BIA inhibitor, suggesting the faster dissolution rate of mild steel in 1.0 M HCl solution at higher temperatures. Meanwhile, the inhibition efficiency decreases with the increase of temperature, which can be attributed to the higher desorption rate than the adsorption rate of BIA inhibitor molecules on mild steel surface. It is reported that the decrease of inhibition efficiency with temperature indicated physical adsorption of inhibitor molecules onto mild steel surface [40]. Therefore, the BIA inhibitor was mainly physical adsorption on the mild steel surface. This result is in good accordance with that deduced from adsorption isotherm. The linear relationship between $log(C_R)$ and $1000/T$ can be derived from Fig.10. According to the Arrhenius equation [41,42], the apparent activation energy (E_a) for mild steel dissolution in 1.0 M HCl solution without and with 200 mg/L BIA inhibitor can be calculated as:

$$\log(C_R) = \frac{-E_a}{2.303RT} + \log(A) \qquad (9)$$

Where R is the universal gas constant, T is absolute temperature, A is the pre-exponential factor.

Table 5. The weight loss parameters for mild steel dissolution in 1.0 M HCl solution without and with 200 mg/L BIA inhibitor at different temperatures.

Temperature (°C)	Blank *CR* (mg cm^{-2} h^{-1})	200 μM *CR* (mg cm^{-2} h^{-1})	η(%)
30	4.78	0.172	96
40	8.45	1.08	87
50	20.3	3.17	84
60	28.5	8.18	71

Moreover, other activation parameters, including enthalpy (ΔH_a^0) and entropy (ΔS_a^0) for mild steel dissolution in 1.0 M HCl solution without and with 200 mg/L BIA inhibitor can be calculated using the transition state equation [43]:

$$C_R = RT / Nh \exp(-\Delta H_a^0 / RT) \exp(\Delta S_a^0 / R) \qquad (10)$$

Where C_R is the corrosion rate at different testing temperature, N is Avogadro's number and h is Plank's constant.

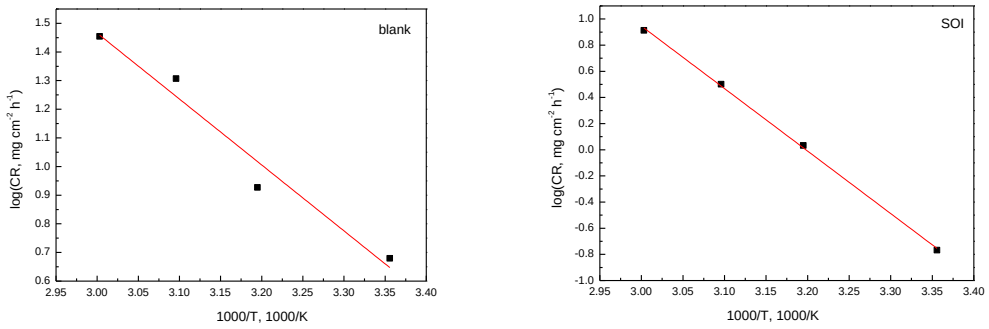

Figure 10. Arrhenius plot of log (C_R) versus 1000/T in the absence and presence of 200 mg/LBIA inhibitor.

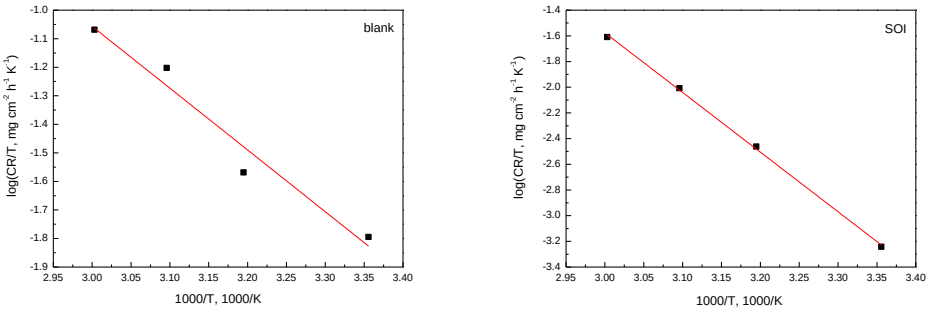

Figure 11. log (C_R/T) versus 1000/T in the absence and presence of 200 mg/LBIA inhibitor.

Table 6. The activation parameters for mild steel in 1.0 M HCl solution without and with 200 mg/L BIA inhibitor.

	1 mol/L HCl		
c (mg/L)	E_a	ΔH_a^0	ΔS_a^0
	KJ mol^{-1}	KJ mol^{-1}	J mol^{-1} K^{-1}
0	44	41	94
200	92	89	-39

The values of E_a at different conditions are summarized in Table 6. The values of E_a obtained with addition of 200 mg/L BIA inhibitor were calculated to be 92 kJ/mol, which was larger than that of 44 kJ/mol for the blank, indicating the physical adsorption mechanism of BIA inhibitor on mild steel surface [44].This conclusion agrees well with that inferred from the Langmuir adsorption isotherm. Meanwhile, the positive value of ΔH_a^0 reveals that the mild steel dissolution process is endothermic and the larger value of ΔH_a^0 in the presence of BIA inhibitor (89 KJ mol^{-1}) compared to the absence (41 KJ mol^{-1}) suggests slower dissolution of mild steel in the presence of 200 mg/L BIA inhibitor. Furthermore, the larger negative value of ΔS_a^0 with addition of 200 mg/L BIA inhibitor is ascribed to decrease in disorder and implies the loss of translation freedom by the adsorption of BIA molecules on mild steel surface.

3.7 Effect of immersion time

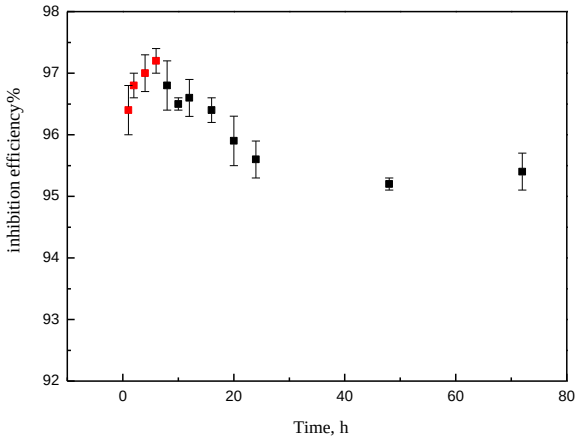

Figure 12. Dependence of inhibition efficiency on immersion time for mild steel corrosion in 1.0 MHCl solution in the presence of 200 mg/L BIA inhibitor.

The effect of immersion time on the inhibition efficiency for mild steel corrosion in 1.0 M HCl solution in the presence of 200 mg/L BIA inhibitor is depicted in Fig.12. It can be seen that the inhibition efficiency slowly increases with increasing immersion time during the initial immersion period from 2 h to 6 h, while decreases with increasing immersion time from 6 h to 72 h. This finding may be explained by the equilibrium of BIA inhibitor adsorption/desorption on mild steel surface at about 6 h. Furthermore, after about 72 h immersion time, the inhibition efficiency is still over 95%, indicating the efficient long-term inhibition performance of BIA inhibitor for mild steel in 1.0 M HCl solution.

Table 7. Inhibition effect of different inhibitors for mild steel in 1.0 M HCl solution reported in the literatures.

Inhibitors	Maxumium IE%	c (g/L)	Long-term effect	Ref.
N-[Morpholin-4-yl(phenyl)methl]acetamide	91.8	2.34	no reported	**[4]**
2-(n-octylamino)-4-(3'-N,N-dimethylamino-propyl) amino-6-(benzothiazole-2-yl)thio-1,3,5-s-triazine	99.3	0.461	no reported	**[5]**
di-triethanolamine siloxane	96	0.322	no reported	**[7]**
3-(4-pyridyl)-2-Amino-1,3,4-triazole	93	0.322	no reported	**[10]**
1-(4-methyl-phenyl)-1H-pyrrole-2,5-dione	97.5	0.187	no reported	**[20]**
S-heterocyclic Schiff base	92.95	4.04	no reported	**[23]**

4-(((4-(bis(pyridine-2-ylmethyl)amino)phenl) imino)methyl)-N,N-diethylaniline	91.9	0.45	no reported	**[28]**
(4-benzothiazole-2-yl-phenyl)-dimethyl-amine	95	0.05	no reported	**[35]**
N-benzyl-N-(2,4-diamino) butyl imidazoline ammonium chloride	96.4	0.20	>95% at 72 h	This work

The comparison of inhibition effect between inhibitors reported in literatures and the present work is shown in Table 7. It is clear that the inhibitor 2-(n-octylamino)-4-(3'-N,N-dimethylamino-propyl)amino-6-(benzothiazole-2-yl)thio-1,3,5-s-triazine exhibited the highest inhibition efficiency of 99.3% at a moderate concentration for mild steel in 1.0 M HCl solution. While some inhibitors showed smaller values of the inhibition efficiency, although with addition of larger concentration [4,23]. It is noticeable that the effect of immersion time on the inhibition efficiency was not reported for most of the studies. Therefore, based on the experimental results, it is rational that the soybean oil based imidazline derivative has the practical potential for protection of mild steel corrosion in 1.0 M HCl solution due to its good inhibition effect and long-term inhibition performance.

4. CONCLUSIONS

Novel imidazoline derivative, named N-benzyl-N-(2,4-diamino) butyl imidazoline ammonium chloride (BIA) based on soybean oil was synthesized and its inhibition behavior for mild steel in 1.0 M HCl was investigated using gravimetric measurements, potentiodynamic polarization, electrochemical impedance spectroscopy (EIS), scanning electron microscopy and energy dispersive spectrum. Results suggested that BIA acted as an efficient inhibitor for mild steel in 1.0 M HCl solution. Gravimetric measurements indicated that the corrosion rate decreased while the inhibition efficiency increased with the increase of inhibitor concentration and the inhibition efficiency showed the maximum value of 96.4% at 200 mg/L. Potentiodynamic polarization results revealed that the BIA compound was a mixed-type inhibitor, and predominantly cathodic.BIA inhibitor was physical adsorption on mild steel surface in 1.0 M HCl solution and the adsorption behavior followed Langmuir adsorption isotherm. Activation and thermodynamic parameters (E_a , ΔH^* , ΔS^*) were also calculated to supply useful information on the correlation between BIA inhibitor molecules and mild steel surface.

ACKNOWLEDGEMENTS
This work was supported by National Natural Science Foundation of China (Project 21403194, 21607011), the Natural Science Foundation of Shandong Province (ZR2019QEM003, ZR2014BQ027,ZR2016BP11), the Major Project of Binzhou University (2017ZDL02), the Science and Technology Development Plan of Binzhou (2013ZC0703), and Scientific Research Fund of Binzhou University (BZXYG1802, BZXYZZJJ201604, BZXYFB20140805).

References

1. C.B. Verma, M.A. Quraishi and A. Singh, *J. Taiwan. Inst. Chem. E.*, 49 (2015) 229.
2. K. Mallaiya, R. Subramaniam, S.S. Srikandan, S. Gowri, N. Rajasekaran and A. Selvaraj, *Electrochim. Acta,* 56 (2011) 3857.
3. N.A. Negma, N.G. Kandile, E.A. Badr and M.A. Mohammed, *Corros. Sci.*, 65 (2012) 94.
4. A. Jamal Abdul Nasser and M. Anwar Sathiq, *Arab. J. Chem.*, 9 (2016) S691.
5. Zhiyong Hu, YanbinMeng, Xuemei Ma, Hailin Zhu, Jun Li, Chao Li and Duanlin Cao, *Corros. Sci.*,112 (2016) 563.
6. M. Karimi, M.M. Shirazi and S. Ayatollahi, *J. Petrol. Sci. Eng.*, 166 (2018) 121.
7. K. Zakaria, A. Hamdy, M.A. Abbas and O.M. Abo-Elenien, *J. Taiwan. Inst. Chem. E.*, 65 (2016) 530.
8. I.B. Obot, S.A. Umoren, Z.M. Gasem, Rami Suleiman and Bassam El Ali, *J. Ind. Eng. Chem.*, 21 (2015) 1328.
9. I.B. Obot and N.O. Obi-Egbedi, *Corros. Sci.*, 52 (2010) 198.
10. KoraySayin, HojatJafari and FarhadMohsenifar, *J. Taiwan. Inst. Chem. E.*, 68 (2016) 431.
11. P.E. Alvarez, M.V. Fiori-Bimbi, A. Neske, S.A. Brandan and C.A. Gervasi, *J. Ind. Eng. Chem.*, 58 (2018) 92.
12. S. Varvara, R. Bostan, O. Bobis, L. Găină, F. Popa, V. Mena and R.M. Souto, *Appl. Surf. Sci.*, 426 (2017) 1100.
13. YujieQiang, Shengtao Zhang, Bochuan Tan and Shijin Chen, *Corros. Sci.*, 133 (2018) 6.
14. A. Ehsani, M.G. Mahjani, M. Hosseini, R. Safari, R. Moshrefi and H.M. Shiri, *J. Colloid. Interf. Sci.*, 490 (2017) 444.
15. M. Mobin and M. Rizvi, *Carbohyd. Polym.*, 160 (2017) 172.
16. A.S. Fouda, A.S. Abousalem and G.Y. El-Ewady, *Int. J. Ind. Chem.*, 8 (2017) 61.
17. Y. Chen, Y.Y. Jiang, H. Chen, Z. Zhang, J.Q. Zhang and C.N. Cao, *J. Am. Oil. Chem. Soc*., 90 (2013) 1387.
18. Z.N. Yang, Y.W. Liu and Y. Chen, *Int. J. Electrochem. Sci.*, 13 (2018) 514.
19. A. Khadraoui, A. Khelifa, M. Hadjmeliani, R. Mehdaoui, K. Hachama, A. Tidu, Z. Azari, I.B. Obot and A. Zarrouk, *J. Mol. Liq.*, 216 (2016) 724..
20. A. Zarrouk, B. Hammouti, T. Lakhlifi, M. Traisnel, H. Vezin and F. Bentiss, *Corros. Sci.*, 90 (2015) 572.
21. YujieQiang, Shengtao Zhang, Lei Guo, Shenying Xu, Li Feng, Ime B. Obot and Shijin Chen, *J. Clean. Prod.*, 152 (2017) 17.
22. M. Bahrami, S. Hosseini and P. Pilvar, *Corros. Sci.*, 52 (2010) 2793.
23. D. Daoud, T. Douadi, H. Hamani, S. Chafaa and M. Al-Noaimi, *Corros. Sci.*, 94 (2015) 21.
24. Y.W. Liu, Y. Chen, X.H. Chen, Z.N. Yang, Y. Xie and Z. Zhang, *J. Alloy. Compd.*, 758 (2018) 184.
25. D.H. van der Weijde, E.P.M. van Westing and J.H.W.de Wit, *Corros. Sci.*, 36 (1994) 643
26. P. Campestrini, E.P.M van Westing and J.H.W de Wit, *Electrochim. Acta*,46(2001) 2631.
27. R. Solmaz, G. Kardas, M. Culha, B. Yazici and M. Erbil. *Electrochim. Acta*, 53 (2008) 5941.
28. Yan Ji, Bin Xu, Weinan Gong, Xueqiong Zhang, XiaodongJin, Wenbo Ning, Yue Meng, Wenzhong Yang and Yizhong Chen, *J. Taiwan. Inst. Chem. E.*, 66 (2016) 301.
29. N.D. Nam, Q.V. Bui, M. Mathesh, M.Y.J. Tan and M. Forsyth, *Corros. Sci.*, 76 (2013) 257.
30. S.S. Abd El Rehim, M.A.M. Ibrahim and K.F. Khalid, *Mater. Chem. Phys.*, 70 (2001) 268.
31. Y. Chen, X.H. Chen, Y.W. Liu, Z.N. Yang and Z. Zhang, *J. Chem. Thermodynamics*, 126 (2018) 147.
32. R. Mohan, K. Ramya, K.K. Anupama and A. Joseph, *J. Mol. Liq.*, 220 (2016) 707.
33. Zhiyong Hu, YanbinMeng, Xuemei Ma, Hailin Zhu, Jun Li, Chao Li and Duanlin Gao, *Corros. Sci.*, 112 (2016) 563.
34. G. Ji, S. Anjum, S. Sundaram and R. Prakash, *Corros. Sci.*, 90 (2015) 107.

35. Z. Salarvand, M. Amirnasr, M. Talebian and K. Raeissi, *Corros. Sci.*, 114 (2017) 133.
36. A.M. Badiea and K.N. Mohana, *Corros. Sci.*, 51 (2009) 2231.
37. M.H. Hussin, M.J. Kassim, N.N. Razali, N.H. Dahon and D. Nasshorudin, *Arab. J. Chem.*, 9 (2016) S616.
38. R. Solmaz, *Corros. Sci.*, 79 (2014) 169.
39. M. Behpour, S.M. Ghoreishi, N. Soltani, M. Salavati-Niasari, M. Hamadanian and A. Gandomi, *Corros. Sci.*, 50 (2008) 2172.
40. E.E. Oguzie, C. Unaegbu, C.E. Ogukwe, B.N. Okolue and A.I. Onuchukwu, *Mater. Chem. Phys.*, 84 (2004) 363.
41. M. Behpour, S.M. Ghoreishi, N. Soltani and M. Salavati-Niasari, *Corros. Sci.*, 51 (2009) 1073.
42. A.A. Khadom, A.S. Yaro, A. Amir and H. Kadum, *J. Taiwan. Inst. Chem. E.*, 41 (2010) 122.
43. M.A. Quraishi and M.A. Singh, *J. Appl. Electrochem.*, 40 (2010) 1293.
44. L. Larabi, Y. Harek, O. Benali and S. Ghalem, *Prog. Org. Coat.*, 54 (2005) 256.